Cellulose (2021) 28:9187–9206
https://doi.org/10.1007/s10570-021-04109-w

ORIGINAL RESEARCH

Influence of pretreatment and mechanical nanofibrillation energy on properties of nanofibers from Aspen cellulose

A. Balea · E. Fuente · Q. Tarrés · M. Àngels Pèlach · P. Mutjé · M. Delgado-Aguilar · A. Blanco · C. Negro

Received: 19 January 2021 / Accepted: 23 July 2021

Abstract The characteristics of cellulose nanofibers (CNFs) depend on many factors such as the raw material, type and intensity of the pre-treatment, and type and severity of the mechanical defibrillation process. The relationship among factors is complex but crucial in determining the final, fit-for-use CNF properties. This study aims to find the relationship between the CNF properties morphology, aspect ratio, nanofibrillation yield, transmittance and cationic demand, and the production process using bleached Aspen thermomechanical pulp as the raw material. Five different types of pretreatments were carried out and five different defibrillation intensities of high-pressure homogenization were evaluated. Pretreatments were: PFI refining at 20,000 revolutions, enzymatic hydrolysis with 80 and 240 g of enzyme per ton of dry pulp and TEMPO (2,2,6,6-tetramethylpiperidine-1-oxyl)–mediated oxidation with 5 and 15 mmol of NaClO per gram of dry pulp. From the twenty-five different procedures evaluated, results show that both the pretreatment and the severity of the high-pressure homogenization determined both the fibrillation yield and the CNF morphology. Moreover, the main properties of CNFs (cationic demand, yield, transmittance and aspect ratio) can be estimated from the carboxylic content of the pretreated pulp, which would facilitate the control of the CNF production and their tuning according to the production needs.

Keywords Aspen · Nanocellulose · Enzymatic hydrolysis · TEMPO-mediated oxidation · Refining · High-pressure homogenization

A. Balea · E. Fuente · A. Blanco · C. Negro (✉)
Department of Chemical Engineering and Materials, University Complutense of Madrid, Avda. Complutense s/n, 28040 Madrid, Spain
e-mail: cnegro@ucm.es

Q. Tarrés · M. À. Pèlach · P. Mutjé · M. Delgado-Aguilar
LEPAMAP Research Group, University of Girona, Maria Aurèlia Capmany, 6, 17003 Girona, Spain

Introduction

Different products based on nanocellulose, such as cellulose nanofibers (CNFs), hydrogels, aerogels, filaments, nanopapers and nanowhiskers, have been developed during last decades. The number of studies on new processes to produce new nanocelluloses are increasing (Ewulonu et al. 2019; Xia et al. 2020; Miao et al. 2020; Yu et al. 2020; Liu et al. 2021). The production process determines the obtained product. Nanowhiskers, cellulose nanocrystals, are obtained by means of dissolving amorphous parts of cellulose; bacterial nanocellulose is obtained by fermentation driven by Acetobacter species; and CNF production requires mechanical nanofibrillation to disintegrate the fiber structure into its elemental cellulosic nanofibrils and bundles of several of these. New

processes are being developed to overcome the environmental and economic challenges of nanocellulose production (Balea et al. 2020), as for example: (1) using ionic liquids to dissolve lignin, hemicellulose and cellulose to produce regenerated cellulose and derivative products with different morphologies and properties (Xia et al. 2020) or (2) using streams rich in cellulose, i.e. broke streams, of the paper machines, to produce in situ CNFs for direct application on the paper mill (Balea et al. 2019).

Since CNFs were first produced in 1983 by Turbak et al. (1983), several production processes have been developed. These processes utilize different pretreatments followed by mechanical disintegration. Pretreatments include refining, enzymatic hydrolysis and chemical processes, such as carboxymethylation (TEMPO (2,2,6,6-tetramethylpiperidine-1-oxyl)–mediated oxidation and periodate–chlorite oxidation), cationization, and acidic or basic pretreatments, among others (Blanco et al. 2018; Chaker and Boufi 2015; Henriksson et al. 2007; Isogai 2020; Khalil et al. 2014; Saito et al. 2007; Siro and Plackett 2010; Zambrano et al. 2020). In addition, a wide variety of cellulose sources can be used to produce the nanofibers including non-woody plants, lignocellulosic wastes, marine animals (tunicate), algae, fungi, invertebrates or bacteria, although woody pulps (in particular softwood) are still the most-used raw materials (Blanco et al. 2018; Jonoobi et al. 2015; Rajinipriya et al. 2018). The potential of lignocellulosic wastes as a source of cellulose, hemicellulose and lignin derivatives is increasing because they are a cheap and a worldly available renewable raw material alternative to petroleum for the manufacture of valuable products, such as biodegradable films and composites, nanomaterials, chemical basic products, etc. The potential increases as the development of new low environmental impact fractionation processes and new lignocellulosic nanomaterials, which does not require lignin removal, are developed (Ewulonu et al. 2019; Miao et al. 2020; Yu et al. 2020; Liu et al. 2021). This also contributes to increase of interest in using alternative wood plants, for example Aspen, which is not widely used for pulp and paper production, but that could be concerning for nanocelluloses and lignonanocelluloses production.

Given the high number of possibilities involved in CNF production, there is a fragmentation of knowledge, and this complicates the prediction of CNF properties. There are three major independent factors that influence CNF characteristics: (1) chemical composition, morphology, swelling ability and crystallinity of the cellulose source; (2) type of the pretreatment and its intensity and (3) mechanical defibrillation process and its severity. Moreover, the morphology and chemical properties of CNFs should be also linked with their final application developing the concept of nanocellulose-fit-for-use.

It is well-known that more severe mechanical defibrillation treatments can produce an increased fraction of the nanofibrillated material. For example, in high-pressure homogenization (HPH), the number of passes and the pressure applied can be controlled to determine the extent of the mechanical treatment, but this does not necessarily determine the fibrillation effect, because it also depends on the other two factors above. Moreover, increasing the number of passes at high pressure, to achieve a desirable nanofibrillation degree, leads to a high energy consumption and this is still one of the reasons hindering the CNF industrial production (Balea et al. 2020; Naderi et al. 2015).

The chemical composition of the cellulose source, primarily the cellulose, hemicellulose, lignin and extractive content, has a direct impact on the properties and production requirements of CNFs (Jonoobi et al. 2014; Osong et al. 2016). Several authors have reported that a certain amount of lignin and the preservation of hemicelluloses facilitate the mechanical fibrillation and, thus, reduce energy consumption (Chaker et al. 2013; Delgado-Aguilar et al. 2016; Ferrer et al. 2012; Spence et al. 2010a, b; Tarres et al. 2017; Espinosa et al. 2020). Ferrer et al. (2012) found that residual amounts of lignin stabilize the radicals formed during homogenization, which enhances the fibrillation step. However, Albornoz-Palma et al. (2020) suggest that the presence of lignin in the pulp reduces the fibrillation yield and affects the CNF properties, because lignin nanoparticles, produced during homogenization, act as cement for the nanofibrils. Several authors have reported that an appropriate balance between hemicelluloses, lignin and other polysaccharides is beneficial for the mechanical fibrillation because the formation of fiber bundles and the aggregation of micro and/or nanofibers are notably reduced (Chaker et al. 2013; Tarres et al. 2017). In fact, the sensitivity of polysaccharides to defibrillation treatments depends strongly on their structure: globular branched structures such as gum

arabic are almost unaffected, while linear polymers, such as cellulose, undergo depolymerization (Villay et al. 2012).

Crystallinity of the raw material, which is related to the chemical composition, also affects the efficiency and yield of the pretreatments as well as the final CNF properties (e.g. degree of polymerization). In pulps with lower crystallinity (generally those with increased hemicellulose and lignin contents), part of the NaClO used for TEMPO-mediated oxidation is used for oxidation and polymerization of lignin, reducing the efficiency of the process (Balea et al. 2016c; Ma et al. 2012). In the case of acid hydrolysis pre-treatment, at identical production conditions, the yield increases with the crystallinity of the pulp because mono and disaccharide production is lower as crystalline regions are less susceptible to acid degradation (Zhao et al. 2006). However, it is not the main factor affecting CNF properties after HPH, but there are many other variables involved in the pulp behaviour during HPH treatment, e.g. lignin content, aspect ratio, and surface charged groups, among others.

The main benefit of pretreatment is to reduce the energy demand and to avoid clogging in the subsequent treatments, but pretreatments can have a notable effect on CNF characteristics and behavior. Severe pretreatment affects the integrity of the fibers and generates a large amount of fines, which is a potential problem for the subsequent processing stages (Levanič et al. 2020). Several researchers have demonstrated that CNFs of very high aspect ratio, which demand a high energy consumption, have only marginal increased mechanical strength compared to less fibrillated products (Ang et al. 2019; Balea et al. 2016c).

Nowadays, the manufacturing of products containing CNFs is quite challenging because of their high costs (10–100 USD per dry kg). To make them more competitive in the nanomaterials market it is essential to reduce their price by producing larger quantities or to develop industrial synergies at local level to reduce transport costs. In this scenario, the large range of properties and qualities of CNFs resulting from a certain cellulose source should be deeply investigated to facilitate their implementation in a large number of applications (Isogai 2020; Balea et el. 2021).

The state of the art shows a significant number of papers, published in the last 2 decades, focused on the production and applications of CNFs from bleached kraft hardwood and softwood pulps, mainly eucalyptus and pine pulps (Balea et al. 2016a; Osong et al. 2016). Studies on the use of hardwood pulps are still limited because the hardwood fiber structure is more complex and rigid with the outer secondary wall (S1 layer) restricting the flexibility of the fibers and preventing access to the subjacent inner secondary wall (S2 layer) (Stelte and Sanadi 2009). Therefore, pulp pretreatments are a key when hardwood pulp is used as raw material to produce CNFs (Fukuzumi et al. 2009; Saito et al. 2007) However, so far most researches have studied only a single kind of pulp pretreatment (Balea et al. 2016a; Chen et al. 2017; Isogai et al. 2011; Stelte and Sanadi 2009). A small number of researchers have studied micro or nanofibers from hardwood pulp or lignocellulosic wastes using more than one production scheme (Delgado-Aguilar et al. 2015b; Iglesias et al. 2020; Rol et al. 2017; Zambrano et al. 2020; Espinosa et al. 2020). In consequence, the knowledge is weak and fragmented since it is difficult to compare the studies because the raw material and conditions studied are always different.

Furthermore, Bin et al. (2018) compared the CNFs obtained by TEMPO-mediated oxidation of bleached Aspen pulp with those from bleached spruce pulp after removing fatty acids by means of hydrolysis. They concluded that Aspen pulp was more reactive and chemical pretreatments were easily carried out. However, the size of Aspen CNFs and crystallinity were smaller. This could be controlled by means of optimizing the pretreatment to avoid excessive degradation. Aspen pulp has been considered as a potential raw material for CNF production because its higher reactivity, which reduces pretreatment costs, and the fast growing of the Aspen trees, which promotes renewability. Despite of this, the potential of Aspen pulp has been poorly studied and the influence of different pulp pretreatments on CNF characteristics, when several HPH intensities are applied, is still unknown.

Different CNFs were produced from bleached Aspen thermomechanical pulp (TMP). Five different pretreatments have been studied: mechanical pretreatment (PFI refining at 20,000 revolutions), TEMPO-mediated oxidation with 5 and 15 mmol NaClO per gram of dry pulp at basic pH, and enzymatic hydrolysis with 80 and 240 g of enzyme per ton of dry pulp.

Table 1 Chemical composition of bleached Aspen TMP

Compound	Percentage (wt%)
Cellulose	44.06
Hemicelluloses	20.05
Soluble lignin	5.3
Klason lignin	27.5
Extractives	1.3
Ashes	1.8

Table 2 HPH conditions to produce CNFs

HPH sequence number	Number of cycles		
	300 bar	600 bar	900 bar
1	3	0	0
2	3	1	0
3	3	3	0
4	3	3	1
5	3	3	3

Each pretreated pulp was then treated by HPH at five different conditions, varying the operational pressure and the number of passes. All pretreated pulps have been characterized by measuring their chemical composition and morphological parameters. Finally, the characterization of the obtained CNFs (nanofibrillation yield, transmittance, cationic demand, and aspect ratio) allowed evaluating the effect of the pretreatment and the HPH intensity on the quality of the micro and nanofibers (CMFs/CNFs) obtained.

Materials and methods

Materials

Bleached Aspen TMP (thermo-mechanical pulp with two sulfur and chlorine free bleaching stages) was kindly provided by Heinzel Group. Table 1 shows the chemical composition of bleached Aspen TMP.

Crystallinity index (*CrI*) of raw material was 56% according to the methodology described in "Characterization of the pulps" section. The enzymatic hydrolysis was carried out using the commercial enzyme cocktail Novozym 476, provided by Novozymes A/S (Denmark), that contains 2% of endo-β-1,4-glucanases, with an activity factor of 4500 CNF-CA/g of cellulose. All the chemical reagents used for enzymatic hydrolysis, TEMPO-mediated oxidation pretreatment and CNF characterization were supplied by Sigma Aldrich (Spain).

Cellulose nanofibers production

Pretreatments

Five different pretreatments were applied to the pulp prior to defibrillation process to obtain CNFs with different morphology and properties: (1) mechanical pretreatment by using a PFI-mill refiner at 20,000 revolutions according to the ISO standard 5264-2 (2011); (2) enzymatic hydrolysis of pulp at 5 wt.% consistency with 80 and 240 g of enzyme per ton of dry pulp during 4 h at 50 °C according to the methodology reported by Tarres et al. (2016); and (3) TEMPO-mediated oxidation with 5 and 15 mmol of NaClO per gram of dry pulp at 25 °C and pH 10 using the methodology described by Saito et al. (2007).

High-pressure homogenization

In this study, twenty-five different types of CNFs were produced from the same Aspen pulp and characterized. The nanofibrillation step was carried out by passing the pretreated pulp suspensions (1 wt% of consistency) through a high-pressure homogenizer (PANDA Plus 2000 laboratory homogenizer, Gea Niro Soavi, Italy) using different high-pressure homogenization (HPH) conditions (pressure and number of cycles) as it is summarized in Table 2.

All the produced CMFs/CNFs are named following the nomenclature: Pretreatment_dose-CNF HPH sequence number. For example, CNFs produced by enzymatic hydrolysis pretreatment using an enzyme dosage of 80 g/ton followed by HPH sequence of three passes at 300 bar, three passes at 600 bar and three passes at 900 bar was labeled as Enz_80-CNF-5.

Energy consumption of the HPH process was monitored by means of a Circutor CVM-C10 measuring equipment, which directly returned the consumed energy in real time. The energy consumption was recorded after each HPH cycle and it was referred to the processed dry mass.

Characterization of the pulps

Cellulose, hemicellulose and lignin (insoluble and soluble) of bleached Aspen TMP (Table 1) were determined following NREL/TP-510-42618 laboratory analytical procedure. 0.3 g of dry pulp was hydrolyzed with 3 mL of 72 wt% H_2SO_4 during 1 h in a water bath at 30 °C by stirring the sample every five to ten minutes to ensure even acid to particle contact and uniform hydrolysis. Upon completion of the hydrolysis, 84 g of distilled water was mixed with the sample to eliminate phase separation between high and low concentration acid layers. Then, the sample was placed in an autoclave for 1 h at 121 °C. After completion of the autoclave cycle, the hydrolyzed sample was slowly cool to near room temperature and vacuum filtered. Klason lignin (insoluble) remained in the filter and the soluble lignin was determined by measuring the absorbance of the filtrate in the UV–Vis spectrophotometer at 240 nm. Cellulose and hemicellulose content were also determined from the autoclaved hydrolysis solution. Previously, samples were neutralized with calcium carbonate (to pH 5–6) and they were left to settle. Then, the supernatant was filtered through a 0.2 µm filter and, finally, analyzed with HPLC. Extractives (Table 1) were determined by Soxhlet extraction using acetone as solvent according to TAPPI Method T204. Inorganic content (ashes) was determined by calcination at 525 °C using the standard TAPPI Method T211.

Crystallinity of cellulose can be obtained from different methods, such as X-Ray diffraction (XRD) and different kinds of spectroscopy: FTIR, Near-IR, NMR and FT-Raman, among others (Ahvenainen et al 2016). The most commonly used method is XRD. *CrI* of pulps was determined using a Philips X'Pert MPD X-Ray diffractometer. It is equipped with an autodivergent slit fitted with a graphite monocromator, Cu-Kα radiation and the generator operated at 45 kV and 40 mA and with a wavelength of 1.54 Å. XRD patterns were recorded in a range from 4° to 40° 2θ with a scanning speed of 0.02° each 4 s. Different methods have been developed to obtain *CrI* from the XRD patterns. The simplest one was developed by Segal et al. (1959). Segal's method was used to determine *CrI* according to the Eq. (1).

$$CrI(\%) = \frac{I_{200} - I_{min}}{I_{200}} \times 100 \quad (1)$$

where I_{200} is the intensity of the cellulose (200) diffraction peak plane at 22.5° 2θ and I_{min} is the minimum intensity in the region of 18° 2θ. Background was subtracted from each of the diffractograms. XRD patterns of cellulosic materials are complex due to the complexity of cellulose and the possibility of the presence of different cellulose polymorphisms at the same material (cellulose Iα, Iβ, II, III_I and III_{II}) (French 2014). More accurate, but complex methods such us peak deconvolution and Rietveld methods are preferred in some cases where the peaks of different components or polymorphisms of the cellulosic material can overlap and reduce the accuracy of the determination by Segal method. Although Segal method has limitations due to the overlap of crystalline peaks (French 2020), the absence of cellulose II peak reduces this overlap. The aim of XRD analysis, in this case, was not obtaining the exact value of *CrI* of each pulp but comparing the effect of the different treatments on the crystallinity of the pulp. Therefore, Segal method is suitable enough for comparison purposes in this case.

Morphological analysis was performed with a MorFi Compact analyzer (TechPap, France). Average length weighted in average ($length_w$), diameter (d), coarseness and fines percentage (%) were determined from the Aspen pulps after the mechanical (refining), enzymatic hydrolysis and TEMPO-mediated oxidation pretreatments. Aspect ratio of the pretreated samples was estimated through the gel point measurement based on the methodology developed by Sanchez-Salvador et al. (2020) and Varanasi et al. (2013).

The content of carboxylic groups per gram of the pretreated pulps was determined by conductimetric titration (Balea et al. 2016b; Delgado-Aguilar et al. 2015a, b). A dried sample (0.05–0.1 g) was suspended in 15 mL of 0.01 N HCl solution and stirred during 10 min and then taken to a conductivity sensor. The titration was carried out by adding 0.1 mL of 0.01 N NaOH solution to the suspension and then recording the conductivity data in mS/cm. Finally, the number of carboxylic groups was calculated from the titration curve, conductivity *vs* amount (meq) of NaOH added (Habibi et al. 2006).

Characterization of the CNFs

The methodology for CNF characterization by measuring cationic demand (CD), nanofibrillation yield, transmittance at 600 nm and aspect ratio of the CNF suspensions can be found in the authors' previous works (Balea et al. 2016b; Delgado-Aguilar et al. 2015a, b). CD was measured by back titration in a particle charge detector Mütek PCD04 (BTG Instruments, Weßling, Germany). Nanofibrillation yield was evaluated by centrifuging the CNF suspension to isolate the nanofibrillated fraction (contained in the supernatant) from the non-fibrillated one retained in the sediment. Transmittance of the CNF suspensions was measured using a UV–Vis Shimadzu spectrophotometer UV-160A using distilled water as reference and background. Aspect ratio of the CNFs was determined by the recently methodology developed by Sanchez-Salvador et al. (2020) which modify the traditional gel point methodology by dying the fibers with Crystal Violet to enable the visualization of the fibrils sedimentation and by optimizing the sedimentation time to ensure complete settling.

CNF suspensions were observed with a JEOL JEM 1400 plus Transmission Electron Microscopy (TEM) device, operated at 100 kV accelerating voltage. The CCD camera was an Orius SC200, manufactured by Gatan (Pleasanton, USA), of 2048 × 2048 pixels, with a pixel size of 7.4 microns. Microscopy analysis was carried out at the Spanish National Centre of Electronic Microscopy (CNME) following the methodology recently developed by Campano et al. (2020). Moreover, CNFs and Aspen pulp samples after the pretreatments were observed using a Zeiss Axio Lab.A1 optical microscope and a color microscope camera Zeiss AxioCam ERc 5 s (Carl Zeiss Microscopy GmbH, Göttingen, Germany). The optical images were processed using the ImageJ software package to remove smooth continuous background from the images using the menu command *Process›Subtract background* setting as parameters a rolling ball radius of 50 pixels, a light background and a sliding paraboloid.

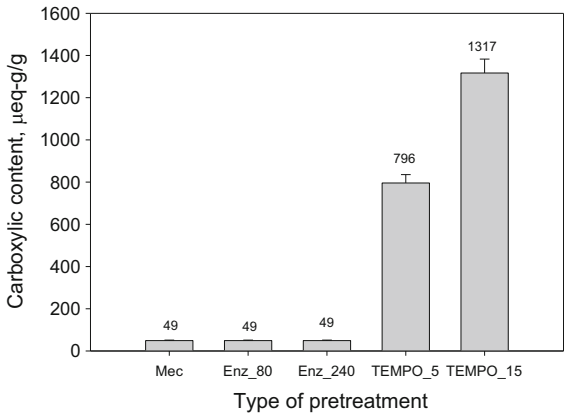

Fig. 1 Carboxylic content of the Aspen fibers after each pretreatment

Results and discussion

Pretreatment effects on fiber morphology and carboxylic content of the pulp

Figure 1 shows that the carboxylic content is determined by the pretreatment nature and its intensity. Only the TEMPO-mediated oxidation was able to produce carboxylic groups in the cellulose chains, as expected, because the enzymatic treatment is designed to break bonds, not to oxidize hydroxyl functional groups. The oxidation grade was not directly proportional to the amount of NaClO used, as the carboxylic content of TEMPO_15 pulp was not three times higher than that for TEMPO_5 pulp. Isogai et al. (2011) has proved that the TEMPO-mediated oxidation was specific for C6 carbon of cellulose. They observed that the oxidation was limited by the available C6 carbon atoms, which were those on the crystalline cellulose microfibrils surface and depended on the cellulose I crystal widths. The maximum oxidation they reached for bleached kraft softwood pulp (BKSP) was around 1300 µeq-g/g, with 10 mmol of NaClO per gram of dry pulp. They obtained a pulp with 1000 µeq-g/g of carboxylic groups when using 5 mmol of NaClO per gram of dry pulp. These results are similar to those obtained from this TEMPO oxidation of bleached Aspen TMP, although this is a hardwood pulp. Recently, El Bakkari et al. (2019) have studied the TEMPO catalyzed CNF production by using bleached Aspen chemi-thermomechanical pulp as raw material. They found that the formation of carboxyl groups reached a peak value of 1335 µeq-g/g when the NaClO concentration was 15 mmol/g, very similar to that shown in Fig. 1. However, higher or lower NaClO dosages reduced the amount of carboxylic groups in the oxidized pulp obtaining values

around 800 μeq-g/g when TEMPO-mediated oxidation was carried out at 5 mmol/g of NaClO (El Bakkari et al. 2019). Moreover, TEMPO catalyzed oxidation of the studied pulp, which is lignin-rich (Table 1), requires higher NaClO dosage to obtain the same oxidation degree than lignin-free pulp, i.e. bleached Kraft pulp with 2.5% klason lignin, (Balea et al. 2016b).

Table 3, Figs. 2 and 3 show the morphology parameters of the fibers, the optical microscope images of the pretreated fibers and their aspect ratio, respectively, caused by different pretreatments. It can be observed that mechanical, enzymatic and TEMPO-mediated oxidation pretreatments have a significant effect on the morphology and the aspect ratio of the fibers. Results from Table 3 show that the three pretreatments reduced fiber length and coarseness while increased the percentage of fines. This is due to the cutting effect of refining, which can be deduced by comparing Fig. 2a and b, or to the degradation of the amorphous part of the cellulose chains and to the deconstruction of the fiber structure resulting in generation of fines. This fact is in agreement with the observations published by Levanič et al. (2020), who observed the evolution of the morphology of bleached eucalyptus pulp during TEMPO-mediated oxidation by means of a Kajaani fiber image analyzer.

The effect on fiber length and coarseness was strongly dependent on the intensity of the pretreatment and it was more affected by TEMPO-mediated oxidation than by enzymatic hydrolysis or mechanical treatment. Mechanical treatment and enzymatic treatment with 80 g/t had a small effect on coarseness, as expected from the degradation of the outer wall of the fiber in both cases, being external fibrillation predominant. Fibrils were observed at the surface of the fibers (Fig. 2b–d). However, TEMPO-mediated oxidation reduced the coarseness by a factor of more than eight, which indicates that fibers were separated into the different microfibrils with a successful internal fibrillation, consistent with the optical images at Fig. 2e and f. In fact, the lack of observed fibers is due to the small size of microfibrils, which are not visible with the optical microscope. The resolution of optical microscope used in this study was around 10 μm; therefore, it only gave information on the sample homogeneity at the micro-scale.

Enzymatic treatment caused a low effect on fiber morphology when an enzyme dose of 80 g/t were used (this can also be observed by comparing Fig. 2a, c). Cellulose fibers have in their structure amorphous and crystalline domains. The first one is the most susceptible for an enzyme or acid hydrolysis while the second one presents lower accessibility due to the protective effect of lignin and hemicellulose (Ribeiro et al. 2019). Although Aspen pulp has been bleached, there is a 33% of residual lignin (Table 1), which could negatively impact the hydrolysis due to the interactions enzyme-lignin or lignin–carbohydrate complex, instead of enzyme-cellulose, affecting the subsequent fibrillation step (Berlin et al. 2006) and reducing the pretreatment efficiency. Some authors have suggested that engineering or a better selection of enzymes with reduced affinity for lignin, so-called "weak-lignin binding enzymes", could be a solution for high-lignin contained pulps (Berlin et al. 2005). Table 3 shows that the increase of enzyme dose was enough to modify the fiber morphology in higher extension than with mechanical refining, which was also observed by Jiang et al. (2020) for bamboo pulp.

While the effect of using 80 g/t of enzyme on the morphology is even lower than the effect of

Table 3 Morphological characteristics of the pulps obtained by mechanical (refining) enzymatic hydrolysis and TEMPO-mediated oxidation pretreatments prior to the high- pressure homogenization

Pretreatment	$Length_w$ (μm)	Diameter (μm)	Coarseness (mg/m)	Fines (%)
Untreated pulp	669 (18)	24.0 (0.3)	0.245 (0.010)	32.5 (4.0)
Mec	480 (21)	22.8 (1.2)	0.245 (0.033)	62.9 (0.9)
Enz_80	604 (39)	23.1 (0.6)	0.245 (0.057)	37.7 (1.8)
Enz_240	205 (28)	23.3 (0.1)	0.170 (0.018)	59.2 (4.6)
TEMPO_5	175 (12)	23.4 (0.3)	0.035 (0.004)	70.5 (2.1)
TEMPO_15	176 (14)	15.8 (0.2)	0.024 (0.004)	78.9 (3.1)

$Length_w$ length weighted in length

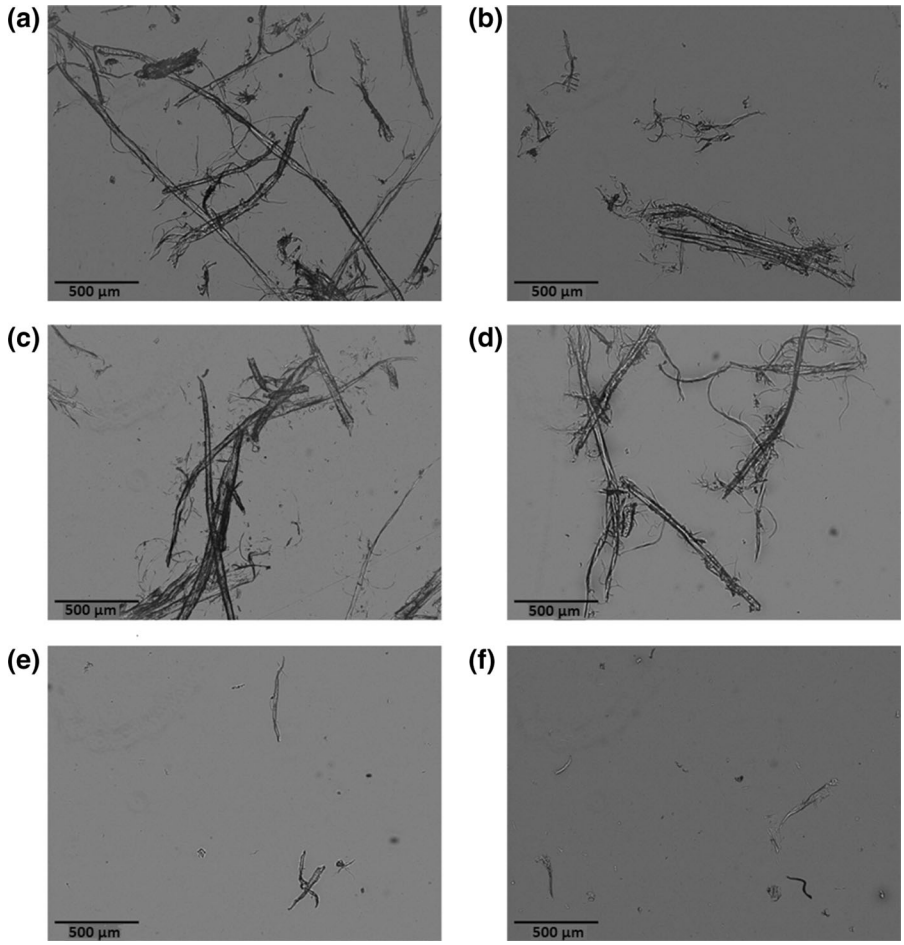

Fig. 2 Optical images of the initial Aspen pulp (without any pretreatment) (**a**) and the pulps after mechanical (**b**); enzymatic hydrolysis with 80 g/t (**c**) and 240 g/t (**d**) and TEMPO-mediated oxidation with 5 and 15 mmol NaClO/g (**e**) and (**f**), respectively

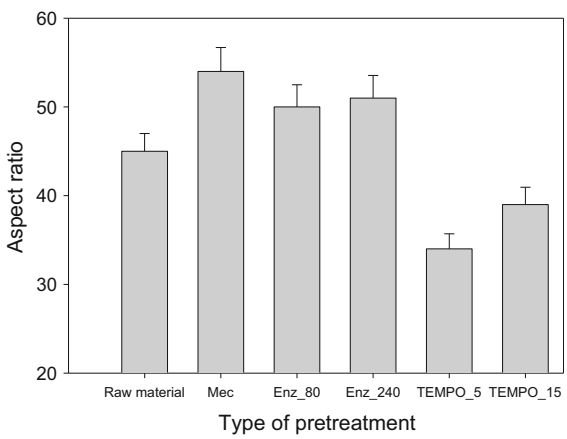

Fig. 3 Aspect ratio of the Aspen fibers after each pre-treatment

mechanical refining, the enzymatic pretreatment with 240 g/t notably decreased the length and coarseness, reaching similar values than those for TEMPO-mediated oxidized pulp, but without such high microfibrillation effect as shown by Fig. 2c and d when comparing to Fig. 2e and f. This is due to the breakage of cellulosic chains by the enzyme as it was observed by Wang et al. (2018) who studied the evolution of the BKSP fiber morphology with the treatment time. They observed that fiber surface was wrinkled, and length was decreased by the enzyme. The enzyme cleaved the cellulose β-1,4 glucosidic bonds even from the crystalline cellulose causing fibrillation and breakage of fibers. It can be observed that although the values of morphological parameters for intense enzymatic pretreated pulp were like those for TEMPO-mediated oxidized pulp, the optical

images are quite different. This is because MorFI equipment analyzes only the fibers that it can detect (lowest detection limit is 5 μm for fiber thickness and 100 μm for fiber length). Then, it calculates the statistics from the population of those fibers, which are the least oxidized in case of TEMPO oxidized pulp, because the others are too small for being detected by the equipment as shown by the Figs. 2e and 2f. This agrees with the low coarseness of TEMPO fibers (Table 3), which indicates that the thickness of a part of the microfibers is lower than 5 μm, being undetected by MorFi equipment. Therefore, other complementary method is required to determine morphological parameters as aspect ratio, which considers all the elements (microfibers, fines and fibers) of the treated pulp.

The gel point has been traditionally used with macroscopic fibers and macrofibrillated fibers, that easily sediment by gravity (Varanasi et al. 2013; Zhang et al. 2012), to determine the aspect ratio of the fibers using the Crowding Number (CN) theory or the Effective Medium Theory (EMT). Figure 3 shows that the aspect ratio of the Aspen fibers, calculated through the gel point using the CN theory, presents important differences depending on the pretreatment that the fibers have suffered. The untreated Aspen pulp has an aspect ratio of 45 and mechanical pretreated fibers show the highest aspect ratio around 55 followed by enzymatic pretreated fibers with an aspect ratio around 50. Both mechanical and enzymatic hydrolysis pretreatments increased the aspect ratio of the fibers compared to the untreated ones due to the higher effect that these pretreatments have on the reduction in the fiber diameter by an external fibrillation of the fibers instead of reducing their length by shortening the cellulose chains. However, the aspect ratio of mechanical and enzymatically pretreated bleached Aspen fibers is about half of the ones determined by Varanasi et al. (2013) for mechanically microfibrillated cellulose supplied from DAICEL Chemical Industries Limited (grade Celish KY-100G) in spite of DAICEL fibers (350 μm length and 15 μm diameter) are shorter than Aspen pulp (Tatsumi et al. 2002). This fact indicates that Aspen fibers are highly separated into the different microfibrils before mechanical defibrillation treatment occurs. The fibers with the lowest aspect ratio, below 40, were extracted from the TEMPO-mediated oxidation pretreatments, which also had the lowest coarseness and the highest fines content according to the results previously discussed (Table 3).

Although gel point measurement was first developed for regular fibers (Martinez et al. 2001), many authors have demonstrated that it is also a convenient parameter to estimate the aspect ratio of microfibers and nanofibers (Raj et al. 2015, 2016a, b; Sanchez-Salvador et al. 2020, 2021). The value of aspect ratio estimated from gel point differs from that calculated from the measured dimensions resulting from MorFi analysis (e.g. 28 for untreated pulp, 9 for Enz_240 and 12 for TEMPO_15), because MorFi equipment is not able to detect the finest particles, such as micro and nanofibers, which have a high aspect ratio. This explains the lower aspect ratios obtained, especially for Enz_240 and TEMPO pretreated pulps, which are the pulps with the highest nanomaterials. Gel point considers the contribution of all the suspended materials, which forms a network. Because of this, it allows estimating a more accurate value for aspect ratio than MorFi analysis at least for pulps containing high number of fines or microfibres.

Figure 4 shows the XRD diffractogram of pretreated pulps. All of them show the typical peaks observed by French (2014) for cellulose Iα, with (110) 16.5° 2θ, (200) 22.5° 2θ and (004) 34.5° 2θ peaks. The cellulose II peaks (1–10) at 12.5° 2θ and (110) at 20° 2θ were not observed (Novo et al. 2015). The five XRD plots were similar, but the (200) peak at 22.5° 2θ became sharper and higher for chemical an enzymatic pretreated pulps. Table 4 summarized the *CrI* calculated by Eq. (1).

Lignin, hemicelluloses and soluble compounds are part of the amorphous phase of the pulp and they contribute with X-ray scattering increasing the width of the (200) peak of crystalline cellulose and the background under the cellulose diffraction region (Agarwal et al. 2013) affecting the XRD patterns and the *CrI*, which can be underestimated. Since lignin degradation consumed part of the NaClO used in TEMPO oxidation, the increase of *CrI* caused by TEMPO oxidation can be due to the delignification rather than the degradation of amorphous cellulose. In fact, the aim of TEMPO-mediated oxidation is not degrading cellulose but modified it by means of selective oxidation of C6 groups without changing the crystallinity of cellulose (Isogai et al. 2011). This explains the similar *CrI* for both TEMPO treated pulps (Ma et al. 2012).

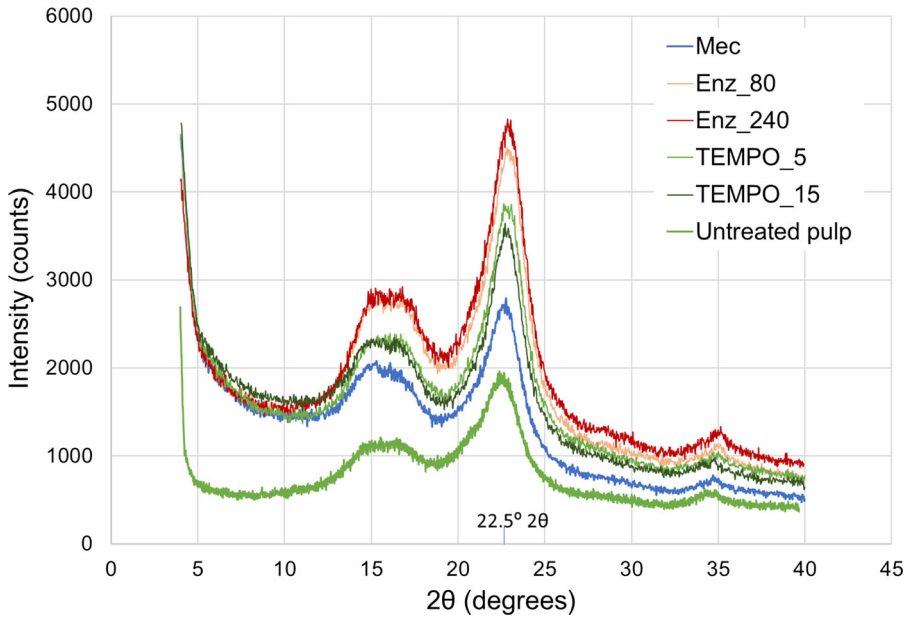

Fig. 4 XRD diffractogram of pulp and pretreated pulps

Table 4 Crystallinity of the pretreated pulp obtained from XRD diffractograms

Pretreatment	*CrI* (%)
Untreated pulp	56.0
Mec	52.5
Enz_80	57.0
Enz_240	58.5
TEMPO_5	58.0
TEMPO_15	58.1

The *CrI* of untreated pulp is according to that obtained by other authors. It is equal to the *CrI* for bleached aspen Kraft pulp (56.8%) obtained by Jin et al. (2014) and to that obtained for chemitermomechanical Aspen pulp after being dried and rewetted once (56%) (Fu et al. 2015). The hornification of fibers in wetting–drying cycles increases the *CrI* by partial recrystallization of cellulose (Fu et al. 2015) Although soft refining increases *CrI* of the pulp due to some hemicelluloses removal, highly severe refining has the opposite effect (Gharehkhani et al. 2015), which is observed in Table 4.

Enzymatic treatment was carried out with endoglucanase that causes β-1,4 glucosidic bonds breakage. Amorphous cellulose is easier to be cleaved by the endoglucanase, which led to an increase in *CrI* and this effect increased with the dose of enzyme.

TEMPO mediated oxidation increased slightly the *CrI* of the pulp. Jin et al. (2014) observed that TEMPO-mediated oxidation followed by high intense ultrasonication and removal of non-nanofibrillated material increased *CrI* up to 80.9%. These results shown that the main contribution to the *CrI* increase was due to the ultrasonication and purification stages since the effect of TEMPO-mediated oxidation is low. The nanocrystals obtained from bleached Aspen kraft pulp by Xu et al. (2013) by acid hydrolysis was also 80%, which indicates that the smallest nanomaterials obtained by Jin et al. (2014) were nanocrystals as they observed by AFM microscopy.

Effect of the pretreatment on the properties of the cellulose nanofibers

Table 5 shows the results of the quantitative characterization of the different CNFs produced by the highest intensity of HPH that corresponds to the sequence 5 as it has previously shown in Table 2. The yield of Mec_CNF-5 was equal to that obtained from bleached spruce TMP with the identical procedure (Serra-Parareda et al. 2021), which indicates that the raw material had not a significant effect on the yield of mechanical obtained CNFs at least with this treatment and HPH sequence.

Table 5 Properties of cellulose nanofibers produced by different pretreatments and followed by HPH (3 passes at 300 bar + 3passes at 600 bar + 3 passes at 900 bar) (sequence 5 of HPH)

	Yield (%)	Transmittance at 600 nm (%)	CD (μeq-g/g)	Aspect ratio -
Mec	22.5	19.3	216	74
Enz_80	23.2	22.4	231	72
Enz_240	26.5	24.7	239	63
TEMPO_5	42.4	39.8	1167	30
TEMPO_15	> 95[a]	90.1	1986	10

[a]After centrifugation, no sediment could be recovered from the bottom of the bottles used during the experiments

CNFs produced from TEMPO-mediated oxidized fibers (TEMPO_5-CNF-5 and TEMPO_15-CNF-5) presented the highest nanofibrillation yield followed by CNFs produced from enzymatic hydrolysis and mechanical refining pretreatments. It is well known that the amount of carboxyl content introduced into the pulp, mainly through TEMPO-mediated oxidation pretreatments (Fig. 1), is a key factor on the final properties of CNFs (Balea et al. 2016c; Besbes et al. 2011; Delgado-Aguilar et al. 2015b). The presence of carboxyl groups in the fiber generates repulsion forces between them, facilitating the defibrillation of the cellulose fibers into nanofibers by shearing forces. Thus, nanofibrillation yield is highly dependent on the amount of negatively charged carboxylic groups formed.

Although the pretreated pulps, by refining and enzymatic hydrolysis, presented the same carboxylic groups content (49 μeq-g/g), the lowest nanofibrillation yield was observed in CNFs produced by refining pretreatment followed by HPH. This demonstrates that the only use of mechanical forces is less efficient for producing nanofibers compared to other pretreatments. These results confirm the observations of Delgado-Aguilar et al. (2015b). Apart of nanofibrillation yield, the transmittance of the CNF suspensions, measured in the visible spectra, is also linked to the degree of nanofibrillation of the produced CNFs. Higher transmittances were observed in TEMPO-oxidized CNFs achieving values around 90% using the highest oxidation degree followed by the highest HPH sequence. However, the use of threefold less of NaClO reduced the transmittance of the CNF suspensions around 3 times. On the other hand, mechanical and enzymatic pretreatments only allowed producing CNFs with transmittance values around 20%.

CD was significantly higher in CNFs produced by TEMPO-mediated oxidation (TEMPO_5-CNF-5 and TEMPO_15-CNF-5) than in CNFs obtained from mechanical and enzymatic pretreatments. The CD results were aligned with the carboxylic content of the pretreated pulp calculated by conductimetric titration (Fig. 1) and the degree of nanofibrillation (nanofibrillation yield or transmittance) of the CNFs obtained (Table 5). As it has been already discussed in the literature (Balea et al. 2016c; Serra et al. 2017), when CNF suspension is mainly formed by high individualized nanofibers, the exposed surface area of cellulose fiber suspension is larger, which increases the number of hydroxyl, aldehyde and carboxylic groups available on the surface of the fibers and, consequently, the amount of cationic polymer required to neutralize them. Furthermore, oxidation increases the percentage of carboxylic and aldehyde groups. Both are translated into higher CD values.

In addition, the relationship between carboxylic groups of the pretreated pulps and the quality of the CNFs (CD, transmittance, nanofibrillation yield and aspect ratio) produced from bleached Aspen pulp is expressed by linear regressions, Eq. (2).

$$y = a + b * CC \quad (2)$$

where CC are the carboxylic groups expressed in μeq-g/g, as shown in Table 6.

These equations allow us to predict the quality of the CNFs that would be obtained after the intense homogenization process for the studied pretreatments. This opens the possibility of on-line control of the CNF main properties and their tuning according to the production needs producing CNFs fit-for-use.

Aspect ratio of TEMPO_5-CNF-5 and TEMPO_15-CNF-5 have been calculated using the methodology described by Sanchez-Salvador et al.

Table 6 Regression results coefficients and standard errors of Eq. (2)

Y	a	b	R^2
CD (μeq-g/g)	152.5	1.3613	0.997
Yield (%)	19.218	0.0506	0.891
Transmittance (%)	17.602	0.0479	0.893
Aspect ratio	71.588	-0.0482	0.974

(2020) which required 10 and 20 sedimentation days, respectively, to ensure a complete settling of the CNF suspensions. This higher sedimentation time is linked to the high fibrillation structure of TEMPO-mediated oxidized CNFs compared to the other pretreatments.

The aspect ratio of the micro/nanofibers, estimated through the gel point, strongly depended on the pulp pretreatment (Table 5). The Mec-CNF-5 had the largest aspect ratio followed by Enz_80-CNF-5, Enz_240-CNF-5 and, finally, the CNFs produced from the TEMPO-oxidized pulps. Both mechanical and enzymatic hydrolysis pretreatments produced CNFs with higher aspect ratio than the fibers of the original Aspen pulp, with an aspect ratio of 45, even without being defibrillated (Fig. 3). Therefore, the higher aspect ratio of the pretreated fibers by refining or enzymatic hydrolysis suggested that macrofibers had been separated into microfibers causing mostly a reduction in the diameter, which predominated over the shortening in the fiber length. This is in accordance with results obtained by Ang et al. (2019) for bleached eucalyptus pulp. In the case of Enz_240, shortening of fibers occurred, but it was not enough to reduce aspect ratio due to the high reduction in fiber diameter and coarseness. Therefore, shorter, but much thinner microfibers were obtained by enzymatic or mechanical pretreatment followed by homogenization. The oxidation of cellulose and the lignin removal caused by NaClO during TEMPO-mediated oxidation increased the sensitivity of cellulose to mechanical forces during HPH process. Therefore, the shortening (cutting) action of an intense HPH treatment increased, which explains the low aspect ratio observed for TEMPO_15-CNF-5. In fact, nanowiskers (with lower aspect ratio than CNFs) can be produced by means of an intense enough TEMPO-mediated oxidation followed by severe HPH process.

Effect of homogenization scheme on morphology and properties of cellulose nanofibers

The homogenization pressure and cycles were varied in this study for the isolation of different CNFs to optimize, in the future, their production depending on the morphology and CNF properties required for a certain application. Optical and TEM micrographs of the twenty-five CNFs produced using different pretreatments of the pulp and sequences of HPH are shown in Figs. 5 and 6, respectively.

Optical microscope images show the different behaviour of the pretreated pulps during the HPH process. Twenty images were taken for each CNF and each image at Fig. 5 is representative from those twenty images. In all the cases, the images represent heterogeneous suspensions with fines and fibers with different morphologies. Mechanical pulp only suffers a soft fibrillation with no significant variation of length during HPH. Fibers were shorter for Enz_240 than for Enz_80 after the HPH sequence 1 treatment, which agrees with the MorFi results shown for pretreated pulps; but more intense HPH cut down the fibers of both pulps while it defibrillated them producing shorter and very thin microfibers. The HPH affected the length and diameter of the Enz_80 and Enz_240 pulp fibers producing microfibers able to be detected by optical microscope and some others too small for being observed at the optical microscope as shown in Fig. 5. In the case of TEMPO pulps, the production of these small undetected microfibers was higher.

The internal fibrillation caused by HPH is clearly shown by Fig. 6 for TEMPO_5 and TEMPO_15, but it is softer in the other cases. Furthermore, small dark spots can be observed in mechanical and enzymatic pretreated pulps. Albornoz-Palma et al. (2020) observed that the HPH treatment causes the deconstruction of lignin and the formation of lignin nanoparticles of around 200 μm, which can be detected by TEM. These particles interfere on the HPH treatment by reducing the defibrillation effect of HPH. This explains the low HPH effect on Mec and Enz_80 pulps. Since the endoglucanases enzymes can interact with lignin (Berlin et al. 2005), reducing their hydrolytic effect, only the treatment with a high dose of enzyme could compensate partially the effect of HPH treatment facilitating the defibrillation of Enz_240 as shown by the image for 5 sequence of the HPH treatment of this pulp.

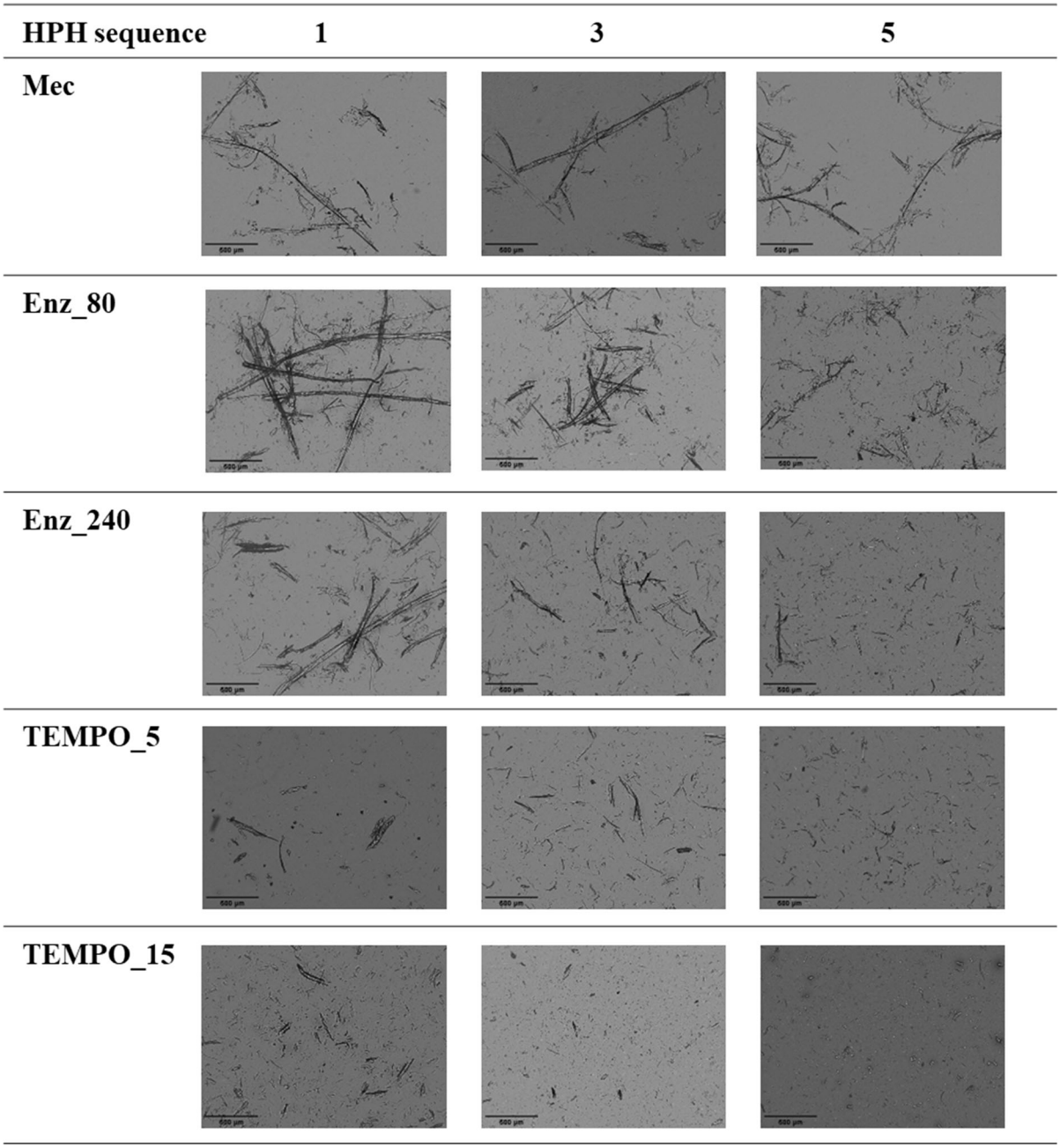

Fig. 5 Optical microscopy images of CNF samples

The effect of temperature increase during the HPH cycles has been recently studied (Park et al. 2019). High temperatures modify the morphology and structure of the fibers favoring rod-like shapes. It is known that the amorphous parts of cellulose are disintegrated with shearing and impact forces via HPH (Jonoobi et al. 2015) and the high temperature of a severe HPH can enhance this effect, increasing the crystallinity of the defibrillated material, which would result in a cellulose nanocrystals product.

Figure 7 shows the nanofibrillation yield, transmittance, CD and aspect ratio of the CNF suspensions. Although mechanical pretreatment by refining causes significant physical changes in the fibers such as

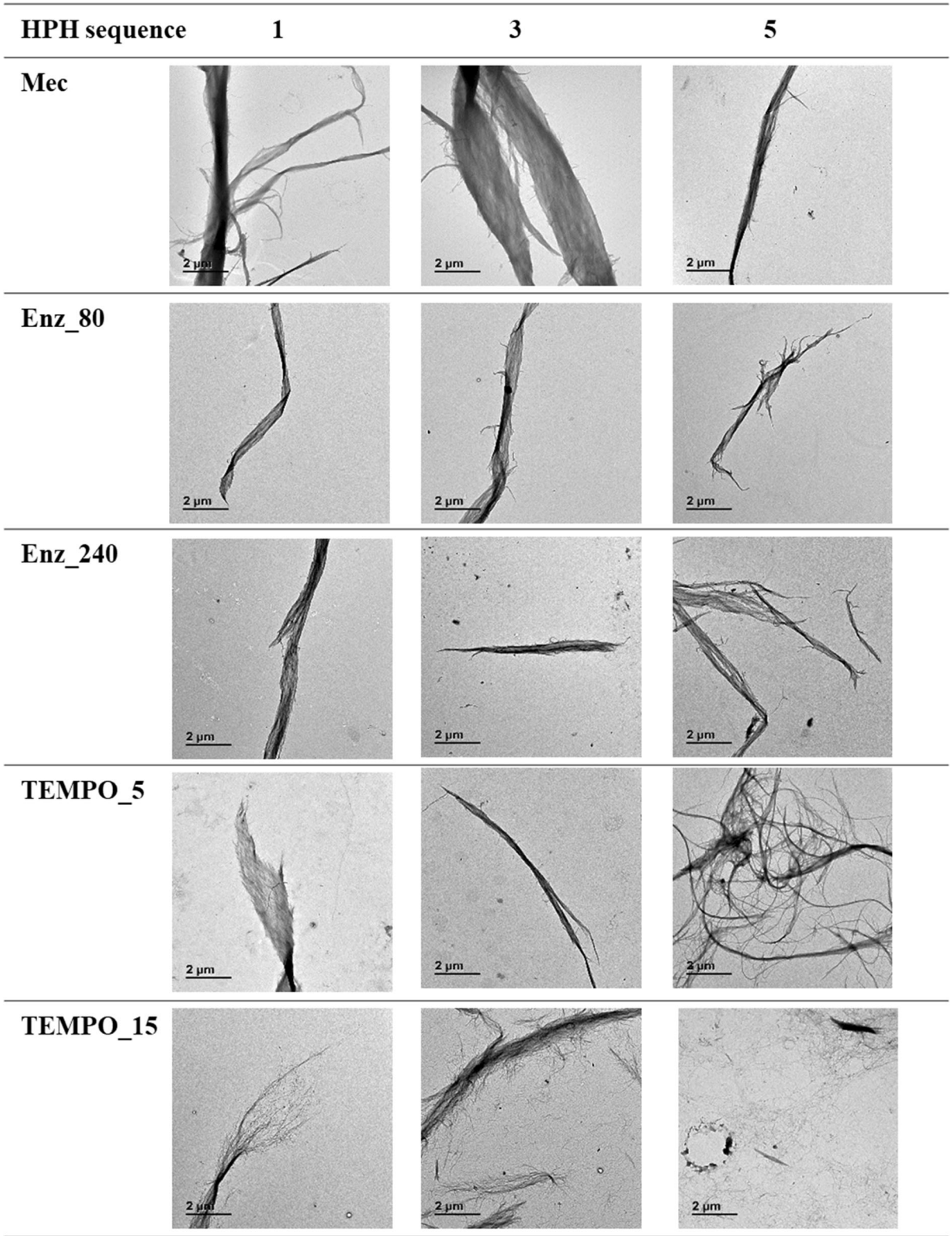

Fig. 6 TEM images of CNF samples

breakage of inner bonds (internal fibrillation), pilling off the fiber surface (external fibrillation), production of fines and shortening of the fibers (Gharehkhani et al. 2015), their impact on the CNF properties is not noticeable, obtaining a low nanofibrillation yield in the subsequent mechanical treatment. On the contrary, the introduction of negative groups in the surface of the fibrils, such as carboxylic groups after TEMPO-mediated oxidation pretreatment, causes repulsion between adjacent fibrils due to electrostatic forces. As consequence, the disruption of fibers into nano and microfibers was favored by the subsequent HPH. Therefore, if highly fibrillated and mainly individualized fibers are required for a certain application neither mechanical nor enzymatic hydrolysis (at the studied conditions) are adequate as pretreatments for bleached Aspen pulp.

For the first time it is demonstrated that the different defibrillation sequences defined in this study follows linear regressions with the nanofibrillation yield that depends on the pretreatment previously applied to the pulp (Eqs. 3–7). This demonstrates that the yield is proportional to the applied energy.

$$\text{Yield}_{\text{Mec}}(\%) = 2.06 + 0.97 \cdot \text{HPHE}, \quad R^2 = 0.995 \tag{3}$$

$$\text{Yield}_{\text{Enz\_80}}(\%) = 4.04 + 1.02 \cdot \text{HPHE}, \quad R^2 = 0.998 \tag{4}$$

$$\text{Yield}_{\text{Enz\_240}}(\%) = 3.02 + 1.35 \cdot \text{HPHE}, \quad R^2 = 0.982 \tag{5}$$

$$\text{Yield}_{\text{TEMPO\_5}}(\%) = 2.72 + 2.44 \cdot \text{HPHE}, \quad R^2 = 0.999 \tag{6}$$

$$\text{Yield}_{\text{TEMPO\_15}}(\%) = 29.03 + 4.08 \cdot \text{HPHE}, \quad R^2 = 0.979 \tag{7}$$

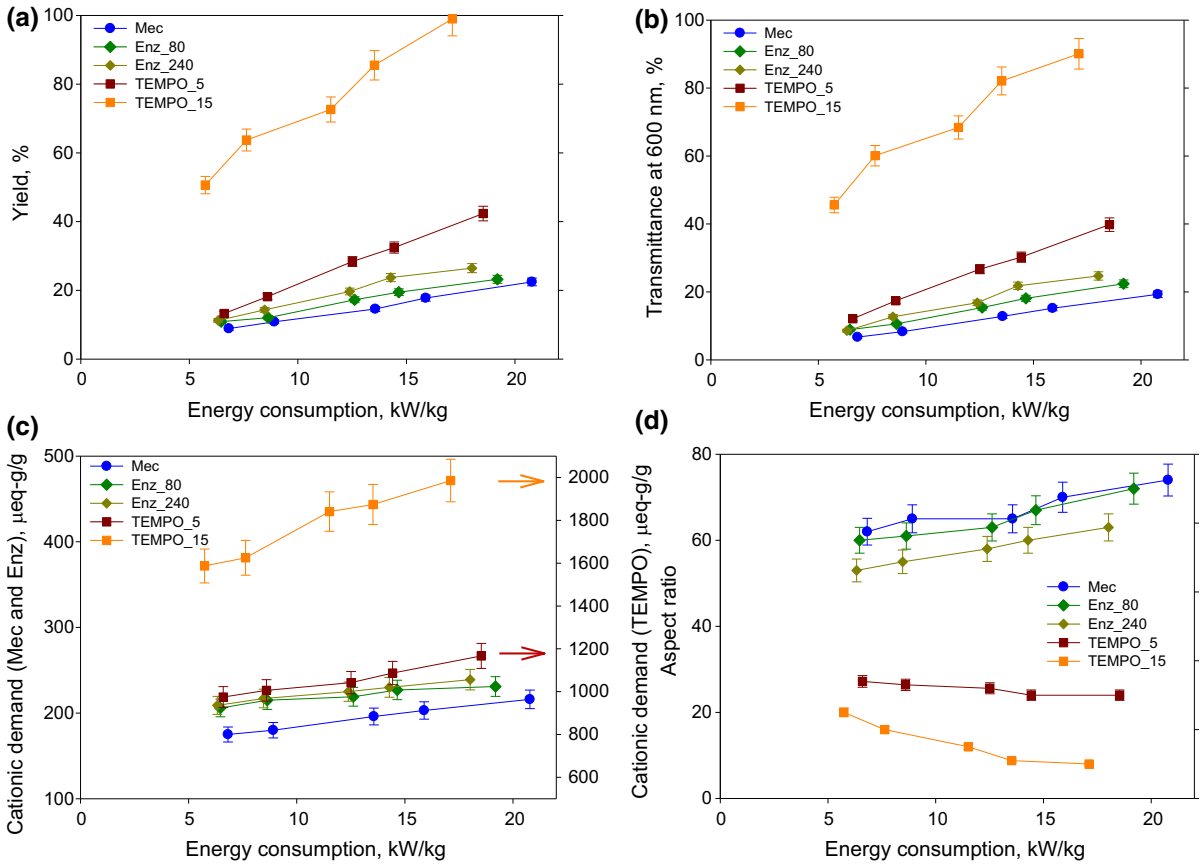

Fig. 7 Nanofibrillation yield (**a**), transmittance (**b**) cationic demand (**c**) and aspect ratio (**d**) of the different CNF suspensions

where HPHE is the total energy consumed per second and per kg of cellulose. It depends on the HPH sequence (Table 2) and on the pulp pretreatment.

Fixing a pulp pretreatment, these linear regressions allow us to determine the most convenient HPH sequence to produce a CNF suspension with a certain nanofibrillation degree. The slope of each curve indicates the sensitivity of the pulp to the HPH treatment. This slope increased slightly by Enz_240 pretreatment. The effect of HPH applied energy on nanofibrillation yield was higher for TEMPO-mediated oxidation pretreated Aspen pulp, as showed by the higher slope of the linear regressions with values of 4.08 (Eq. 7) and 2.44 (Eq. 6) using 15 and 5 mmol NaClO/g, respectively. This is in accordance with the linear relationship previously observed (Table 6) between the yield and carboxylic groups content.

The nanofibrillation yield and transmittance of CNF suspension produced from enzymatic pretreated pulp followed a similar trend with the HPH defibrillation degree than the pulp pretreated by refining being the slopes of the regression lines quite similar. In addition, they were not directly proportional to the amount of enzyme used, as the nanofibrillation yield and transmittance of CNFs produced from of Enz_240 pulp were not three times higher than that produced from Enz_80 pulp.

Two groups of curves can be observed in Fig. 7: (1) those with low yield and low transmittance with low slopes and (2) that for TEMPO_ 15. Even after 3 passes at 300 bar (HPH sequence number 1), the transmittance values of the mechanical and enzymatic pretreated pulp samples are quite low, with values of 6.7, 8.9, 8.6 and 12.1% for Mec-CNF-1, Enz_80-CNF-1 and Enz_240-CNF-1, respectively. The behavior of TEMPO_5 represents an intermediate situation. This is in concordance with the effect of lignin, which is removed due to the presence of the strong oxidant NaClO. Ma et al. (2012) observed that the NaClO removed up to the 13.5% of lignin contained in TMP during TEMPO-mediated oxidation at alkaline conditions and that, despite of this, high carboxylic content (almost 800 μeq/g) was obtained with 5 mmol/g of NaClO. Therefore, the effect of lignin on HPH treatment of TEMPO pulps decreased with the NaClO dose used in the pretreatment. The high delignification caused at TEMPO_15 pulp removed the cementing effect of lignin increasing fibrillation yield and transmittance. Similar results were obtained by Balea et al. (2016c) for maize and rape organosolv pulps. They observed that by bleaching, high nanofibrillated cellulose with similar yield and transmittance than those from TEMPO- mediated oxidation could be obtained.

The yield of Mec-CNF-5 was only 10% higher than that obtained from bleached spruce TMP with the identical procedure (Serra-Parareda et al. 2021), which indicates that the raw material had low effect on the yield of mechanical obtained CNFs with this treatment and HPH sequence. However, differences in yield increased at lower HPH energies. In fact, the obtained yield for Mec-CNF-1 was three times higher (9% for Aspen TMP versus 3% for spruce). Analogue observations can be said for transmittance. This indicates that it is easier to produce mechanical CNFs from Aspen than from spruce. Balea et al. (2019) obtained similar yields from old corrugated carton by means of TEMPO-mediated oxidation and HPH treatment, but the transmittance and cationic demand values were lower.

The aspect ratio of mechanical and enzymatic hydrolysis pretreated pulps increased with increasing homogenization energy, showing that the fiber delamination dominates over fiber shortening (Fig. 7d). This effect has been also observed by Ang et al. (2019) who tried different mechanical treatments and HPH intensities. They observed a close relationship of aspect ratio with the refining revolutions and the number of passes in HPH increasing the aspect ratio up to 173% with the most intense treatment. This does not happen with TEMPO oxidation, which indicates that the HPH of oxidized pulp decreased aspect ratio, which tends to an asymptotic value. This could be due to the degradation of the cellulose and the reduction of polymerization degree, which has been observed by some authors (Villay et al. 2012). Polymerization degree is related to the length of the nanofibers. Polymerization degree of TEMPO oxidized pulp could be more affected by HPH than the pulps treated mechanically or enzymatically and, because of that, the HPH could also reduce the polymerization degree. This explains why there is not a linear relationship between the aspect ratio and HPHE for TEMPO_5 and TEMPO_15, since the effect of HPHE on aspect ratio is the opposite than that for other kinds of pulps and the effect of HPH energy consumption on nanofibers ratio decreases with decreasing their size. However, the

linear relation was evident for mechanical treated pulp (Fig. 7d) because lignin and hemicelluloses protect cellulose chains against cutting and degradation.

The twenty-five different micro/nano fibrillated cellulose suspensions obtained can be divided into three different groups: (1) Microfibrillated cellulose, with high aspect ratio and low fibrillation yield, transmittance, cationic demand and carboxylic groups, when mechanical or soft enzymatic pretreatment were used; (2) Nanofibrillated cellulose with high yield, transmittance, cationic demand and carboxylic groups, but low aspect ratio, when pulp was treated by TEMPO-mediated oxidation with a dose of NaClO of 15 mmol/g; and (3) Nanofibrillated cellulose with high cationic demand and carboxylic groups, but also high aspect ratio, if the dose of NaClO used for TEMPO- mediated oxidation is 5 mmol/g.

Regardless of the pulp pretreatment, nanofibrillation yield of the CNF suspensions clearly correlated with the transmittance values (Fig. 8). Therefore, the transmittance could allow in this case to evaluate the fibrillation extend of the CNF suspensions in a fast way being a robust parameter to be used at industrial scale. This fact is according to Moser et al. (2015) who claimed that transmittance (directly correlated with yield) and turbidity (inversely correlated with yield) are good candidates for easily monitor nanofibrillation during industrial manufacturing. Both properties are fast, easy to measure and with possibility to be implemented on-line.

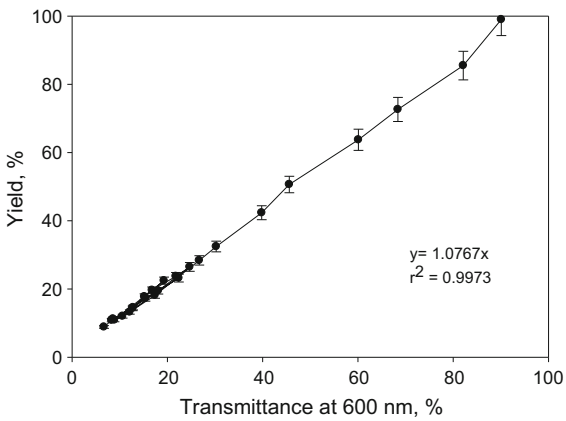

Fig. 8 Nanofibrillation yield vs. transmittance at 600 nm of the different CNF suspensions

Conclusions

Different qualities of nanofibrillated cellulose can be obtained from Aspen TMP by selecting the right pretreatment nature and severity and the optimum HPH intensity. Furthermore, the quality could be predicted and controlled on-line at industrial scale by means of HPH energy consumption. Using Aspen TMP allows increasing the yield compared to some other raw materials, such as spruce, which reduces costs.

The pulp pretreatment highly affects the properties of the obtained nanocellulose and the relation between the HPH energy consumption and the nanocellulose properties. It is concluded that the delignification ability of the pretreatment has a synergic effect with the HPH intensity, determining the nanofibrillation yield and the nanocellulose properties.

Nanocellulose properties (cationic demand, yield, transmittance and aspect ratio) can be estimated from the carboxylic content of the pretreated pulp, through linear relationships. Paying attention to this aspect could make easier and more successful the selection of the optimal pretreatment for CNF production. On the other hand, results show the possibilities of controlling CNF quality at industrial scale based on transmittance, opening the possibility of producing nanocellulose fit-for-use.

Acknowledgements The authors are grateful for the financial support by the Economy and Competitiveness Ministry of Spain (projects CTQ2017-85654-C2-1-R and CTQ2017-85654-C2-2-R) and the Community of Madrid (project S2018/EMT-4459; RETO-PROSOST2-CM). In addition, authors would like to thank to the Spanish National Centre of Electronic Microscopy for the support during TEM images acquisition.

Funding Open Access funding provided thanks to the CRUE-CSIC agreement with Springer Nature. This research has been supported by Economy and Competitiveness Ministry of Spain (Projects CTQ2017-85654-C2-1-R and CTQ2017-85654-C2-2-R) and the Community of Madrid (Project S2018/EMT-4459-RETO-PROSOST2-CM).

Availability of data and material The data sets analyzed during the current study are available from the corresponding author on reasonable request.

Code availability Not applicable.

Declarations

Conflict of interest There is not conflicts of interest.

Human and animal rights This article does not contain any studies with human participants or animals performed by any of the authors.

References

Agarwal UP, Reiner RR, Ralph SA (2013) Estimation of cellulose crystallinity of lignocelluloses using near-IR FT-Raman spectroscopy and comparison of the Raman and Segal-WAXS methods. J Agric Food Chem 61(1):103–113

Ahvenainen P, Kontro I, Svedström K (2016) Comparison of sample crystallinity determination methods by X-ray diffraction for challenging cellulose I materials. Cellulose 23:1073–1086

Albornoz-Palma G, Ching D, Valerio O, Mendonça RT, Pereira M (2020) Effect of lignin and hemicellulose on the properties of lignocellulose nanofibril suspensions. Cellulose 27:10631–10647

Ang S, Haritos V, Batchelor W (2019) Effect of refining and homogenization on nanocellulose fiber development, sheet strength and energy consumption. Cellulose 26:4767–4786

Balea A, Blanco A, Monte MC, Merayo N, Negro C (2016a) Effect of bleached eucalyptus and pine cellulose nanofibers on the physico-mechanical properties of cartonboard. BioRresources 11:8123–8138. https://doi.org/10.15376/biores.11.4.8123-8138

Balea A, Merayo N, Fuente E, Delgado-Aguilar M, Mutje P, Blanco A, Negro C (2016b) Valorization of corn stalk by the production of cellulose nanofibers to improve recycled paper properties. BioResources 11:3416–3431

Balea A, Merayo N, Fuente E, Negro C, Blanco A (2016c) Assessing the influence of refining, bleaching and TEMPO-mediated oxidation on the production of more sustainable cellulose nanofibers and their application as paper additives. Ind Crop Prod 97:374–387

Balea A, Sanchez-Salvador JL, Monte MC, Merayo N, Negro C, Blanco A (2019) In situ production and application of cellulose nanofibers to improve recycled paper production. Molecules 24:1800

Balea A, Monte MC, Merayo N, Campano C, Negro C, Blanco A (2020) Industrial application of nanocelluloses in papermaking: a review of challenges, technical solutions, and market perspectives. Molecules 25:526

Balea A, Blanco A, Delgado-Aguilar M, Monte MC, Tarres Q, Fuente E, Mutje P, Negro C (2021) Nanocellulose characterization challenges. BioResources. https://doi.org/10.15376/biores.16.2.Balea

Berlin A, Gilkes N, Kurabi A, Bura R, Tu M, Kilburn D, Saddler J (2005) Weak lignin-binding enzymes. Appl Biochem Biotechnol 121:163–170

Berlin A, Balakshin M, Gilkes N, Kadla J, Maximenko V, Kubo S, Saddler J (2006) Inhibition of cellulase, xylanase and beta-glucosidase activities by softwood lignin preparations. J Biotechnol 125:198–209. https://doi.org/10.1016/j.jbiotec.2006.02.021

Besbes I, Alila S, Boufi S (2011) Nanofibrillated cellulose from TEMPO-oxidized eucalyptus fibres: effect of the carboxyl content. Carbohydr Polym 84:975–983. https://doi.org/10.1016/j.carbpol.2010.12.052

Bin L, Yang XW, Dennis K (2018) Comparable characterization of nanocellulose extracted from bleached softwood and hardwood pulps. Paper Biomater 3:35

Blanco A, Monte MC, Campano C, Balea A, Merayo N, Negro C (2018) Nanocellulose for industrial use: cellulose nanofibers (CNF), cellulose nanocrystals (CNC), and bacterial cellulose (BC). In: Hussain CM (ed) Handbook of nanomaterials for industrial applications. Elsevier, Amsterdam, pp 74–126

Campano C, Balea A, Blanco Á, Negro C (2020) A reproducible method to characterize the bulk morphology of cellulose nanocrystals and nanofibers by transmission electron microscopy. Cellulose 27:4871–4887

Chaker A, Boufi S (2015) Cationic nanofibrillar cellulose with high antibacterial properties. Carbohydr Polym 131:224–232

Chaker A, Alila S, Mutje P, Vilar MR, Boufi S (2013) Key role of the hemicellulose content and the cell morphology on the nanofibrillation effectiveness of cellulose pulps. Cellulose 20:2863–2875. https://doi.org/10.1007/s10570-013-0036-y

Chen Y, Geng B, Ru J, Tong C, Liu H, Chen J (2017) Comparative characteristics of TEMPO-oxidized cellulose nanofibers and resulting nanopapers from bamboo, softwood, and hardwood pulps. Cellulose 24:4831–4844

Delgado-Aguilar M, Gonzalez I, Pelach MA, De La Fuente E, Negro C, Mutje P (2015a) Improvement of deinked old newspaper/old magazine pulp suspensions by means of nanofibrillated cellulose addition. Cellulose 22:789–802. https://doi.org/10.1007/s10570-014-0473-2

Delgado-Aguilar M, Gonzalez I, Tarres Q, Alcala M, Pelach MA, Mutje P (2015b) Approaching a low-cost production of cellulose nanofibers for papermaking applications. BioResources 10:5345–5355

Delgado-Aguilar M, Gonzalez I, Tarres Q, Pelach MA, Alcala M, Mutje P (2016) The key role of lignin in the production of low-cost lignocellulosic nanofibres for papermaking applications Ind Crop. Prod 86:295–300. https://doi.org/10.1016/j.indcrop.2016.04.010

El Bakkari M, Bindiganavile V, Goncalves J, Boluk Y (2019) Preparation of cellulose nanofibers by TEMPO-oxidation

of bleached chemi-thermomechanical pulp for cement applications. Carbohydr Polym 203:238–245
Espinosa E, Rol F, Bras J, Rodríguez A (2020) Use of multifactorial analysis to determine the quality of cellulose nanofibers: effect of nanofibrillation treatment and residual lignin content. Cellulose 27:10689–10705
Ewulonu CM, Liu X, Wu M, Yong H (2019) Lignin-containing cellulose nanomaterials: a promising new nanomaterial for numerous applications. J Bioresour Bioprod 4:3–10
Ferrer A, Quintana E, Filpponen I, Solala I, Vidal T, Rodríguez A, Rojas OJ (2012) Effect of residual lignin and heteropolysaccharides in nanofibrillar cellulose and nanopaper from wood fibers. Cellulose 19:2179–2193. https://doi.org/10.1007/s10570-012-9788-z
French AD (2014) Idealized powder diffraction patterns for cellulose polymorphs. Cellulose 21:885–896
French AD (2020) Increment in evolution of cellulose crystallinity analysis. Cellulose 27:5445–5448. https://doi.org/10.1007/s10570-020-03172-z
Fu Y, Wang R, Li D, Wang Z, Zhang F, Meng Q, Qin M (2015) Changes in the microstructure and properties of aspen chemithermomechanical pulp fibres during recycling. Carbohydr Polym 117:862–868
Fukuzumi H, Saito T, Wata T, Kumamoto Y, Isogai A (2009) Transparent and high gas barrier films of cellulose nanofibers prepared by TEMPO-mediated oxidation. Biomacromolecules 10(1):162–165
Gharehkhani S, Sadeghinezhad E, Kazi SN, Yarmand H, Badarudin A, Safaei MR, Zubir MNM (2015) Basic effects of pulp refining on fiber properties—a review. Carbohydr Polym 115:785–803
Habibi Y, Chanzy H, Vignon MR (2006) TEMPO-mediated surface oxidation of cellulose whiskers. Cellulose 13:679–687. https://doi.org/10.1007/s10570-006-9075-y
Henriksson M, Henriksson G, Berglund LA, Lindstrom T (2007) An environmentally friendly method for enzyme-assisted preparation of microfibrillated cellulose (MFC) nanofibers. Eur Polym J 43:3434–3441. https://doi.org/10.1016/j.eurpolymj.2007.05.038
Iglesias MC, Gomez-Maldonado D, Via BK, Jiang Z, Peresin MS (2020) Pulping processes and their effects on cellulose fibers and nanofibrillated cellulose properties: a review. For Prod J 70:10–21
Isogai A (2020) Emerging nanocellulose technologies: recent developments. Adv Mater 33:2000630
Isogai A, Saito T, Fukuzumi H (2011) TEMPO-oxidized cellulose nanofibers. Nanoscale 3:71–85. https://doi.org/10.1039/c0nr00583e
Jiang J, Chen H, Liu L, Yu J, Fan Y, Saito T, Isogai A (2020) Influence of chemical and enzymatic TEMPO-mediated oxidation on chemical structure and nanofibrillation of lignocellulose. ACS Sustain Chem Eng 8:14198–14206
Jin L, Wei Y, Xu Q, Yao W, Cheng Z (2014) Cellulose nanofibers prepared from TEMPO-oxidation of kraft pulp and its flocculation effect on kaolin clay. J Appl Polym Sci 131(12):40450
Jonoobi M, Mathew AP, Oksman K (2014) Natural resources and residues for production of bionanomaterials. In: Mathew AP, Oksman K (eds) Handbook of green materials. 1 Bionanomaterials: separation processes, characterization and properties. World Scientific, London, pp 19–33
Jonoobi M, Oladi R, Davoudpour Y, Oksman K, Dufresne A, Hamzeh Y, Davoodi R (2015) Different preparation methods and properties of nanostructured cellulose from various natural resources and residues: a review. Cellulose 22:935–969. https://doi.org/10.1007/s10570-015-0551-0
Khalil H, Davoudpour Y, Islam MN, Mustapha A, Sudesh K, Dungani R, Jawaid M (2014) Production and modification of nanofibrillated cellulose using various mechanical processes: a review. Carbohydr Polym 99:649–665. https://doi.org/10.1016/j.carbpol.2013.08.069
Levanič J, Šenk VP, Nadrah P, Poljanšek I, Oven P, Haapala A (2020) Analyzing TEMPO-oxidized cellulose fiber morphology: new insights into optimization of the oxidation process and nanocellulose dispersion quality. ACS Sustain Chem Eng 8(48):17752–17762
Liu Q, He WQ, Aguedo M, Xia X, Bai WB, Dong YY, Song JQ, Richel A, Goffin D (2021) Microwave-assisted alkali hydrolysis for cellulose isolation from wheat straw: influence of reaction conditions and non-thermal effects of microwave. Carbohydr Polym 253:117170
Ma P, Fu S, Zhai H, Law K, Daneault C (2012) Influence of TEMPO-mediated oxidation on the lignin of thermomechanical pulp. Bioresour Technol 118:607–610
Martinez DM, Buckley K, Jivan S, Lindstrom A, Thiruvengadaswamy R, Olson JA, Ruth TJ, Kerekes RJ (2001) Characterizing the mobility of papermaking fibres during sedimentation. In: The science of papermaking: transactions of the 12th fundamental research symposium, Oxford. The Pulp and Paper Fundamental Research Society, Bury, pp 225–254
Miao X, Lin J, Bian F (2020) Utilization of discarded crop straw to produce cellulose nanofibrils and their assemblies. J Bioresour Bioprod 5:26–36
Moser C, Lindström ME, Henriksson G (2015) Toward industrially feasible methods for following the process of manufacturing cellulose nanofibers. BioResources 10:2360–2375
Naderi A, Lindström T, Sundström J (2015) Repeated homogenization, a route for decreasing the energy consumption in the manufacturing process of carboxymethylated nanofibrillated cellulose? Cellulose 22:1147–1157
Novo LP, Bras J, García A, Belgacem N, Curvelo AA (2015) Subcritical water: a method for green production of cellulose nanocrystals. ACS Sustain Chem Eng 3(11):2839–2846
Osong SH, Norgren S, Engstrand P (2016) Processing of wood-based microfibrillated cellulose, and applications relating to papermaking: a review. Cellulose 23:93–123
Park N-M, Choi S, Oh JE, Hwang DY (2019) Facile extraction of cellulose nanocrystals. Carbohydr Polym 223:115114
Raj P, Varanasi S, Batchelor W, Garnier G (2015) Effect of cationic polyacrylamide on the processing and properties of nanocellulose films. J Colloid Interface Sci 447:113–119
Raj P, Batchelor W, Blanco A, de la Fuente E, Negro C, Garnier G (2016a) Effect of polyelectrolyte morphology and adsorption on the mechanism of nanocellulose flocculation. J Colloid Interface Sci 481:158–167
Raj P, Mayahi A, Lahtinen P, Varanasi S, Garnier G, Martin D, Batchelor W (2016b) Gel point as a measure of cellulose nanofibre quality and feedstock development with mechanical energy. Cellulose 23:3051–3064

Rajinipriya M, Nagalakshmaiah M, Robert M, Elkoun S (2018) Importance of agricultural and industrial waste in the field of nanocellulose and recent industrial developments of wood based nanocellulose: a review. ACS Sustain Chem Eng 6:2807–2828

Ribeiro RS, Pohlmann BC, Calado V, Bojorge N, Pereira N Jr (2019) Production of nanocellulose by enzymatic hydrolysis: trends and challenges. Eng Life Sci 19:279–291

Rol F et al (2017) Pilot-scale twin screw extrusion and chemical pretreatment as an energy-efficient method for the production of nanofibrillated cellulose at high solid content. ACS Sustain Chem Eng 5:6524–6531

Saito T, Kimura S, Nishiyama Y, Isogai A (2007) Cellulose nanofibers prepared by TEMPO-mediated oxidation of native cellulose. Biomacromolecules. https://doi.org/10.1021/bm0703970

Sanchez-Salvador JL, Monte MC, Batchelor W, Garnier G, Negro C, Blanco A (2020) Characterizing highly fibrillated nanocellulose by modifying the gel point methodology. Carbohydr Polym 227:115340

Sanchez-Salvador JL, Monte MC, Negro C, Batchelor W, Garnier G, Blanco A (2021) Simplification of gel point characterization of cellulose nano and microfiber suspensions. Cellulose. https://doi.org/10.1007/s10570-021-04003-5

Segal L, Creely JJ, Martin AE, Conrad CM (1959) An empirical method for estimating the degree of crystallinity of native cellulose using the X-Ray diffractometer. Texti Res J 29:786–794. https://doi.org/10.1177/004051755902901003

Serra A, González I, Oliver-Ortega H, Tarrès Q, Delgado-Aguilar M, Mutjé P (2017) Reducing the amount of catalyst in TEMPO-oxidized cellulose nanofibers: effect on properties and cost. Polymers 9:557

Serra-Parareda F, Aguado R, Tarrés Q, Mutjé P, Delgado-Aguilar M (2021) Chemical-free production of lignocellulosic micro-and nanofibers from high-yield pulps: synergies, performance, and feasibility. J Clean Prod 313:127914

Siro I, Plackett D (2010) Microfibrillated cellulose and new nanocomposite materials: a review. Cellulose 17:459–494. https://doi.org/10.1007/s10570-010-9405-y

Spence KL, Venditti RA, Habibi Y, Rojas OJ, Pawlak JJ (2010a) The effect of chemical composition on microfibrillar cellulose films from wood pulps: mechanical processing and physical properties. Bioresour Technol 101:5961–5968. https://doi.org/10.1016/j.biortech.2010.02.104

Spence KL, Venditti RA, Rojas OJ, Habibi Y, Pawlak JJ (2010b) The effect of chemical composition on microfibrillar cellulose films from wood pulps: water interactions and physical properties for packaging applications. Cellulose 17:835–848. https://doi.org/10.1007/s10570-010-9424-8

Stelte W, Sanadi AR (2009) Preparation and characterization of cellulose nanofibers from two commercial hardwood and softwood pulps. Ind Eng Chem Res 48:11211–11219. https://doi.org/10.1021/ie9011672

Tarres Q, Saguer E, Pelach MA, Alcala M, Delgado-Aguilar M, Mutje P (2016) The feasibility of incorporating cellulose micro/nanofibers in papermaking processes: the relevance of enzymatic hydrolysis. Cellulose 23:1433–1445. https://doi.org/10.1007/s10570-016-0889-y

Tarres Q, Ehman NV, Vallejos ME, Area MC, Delgado-Aguilar M, Mutje P (2017) Lignocellulosic nanofibers from triticale straw: the influence of hemicelluloses and lignin in their production and properties. Carbohydr Polym 163:20–27. https://doi.org/10.1016/j.carbpol.2017.01.017

Tatsumi D, Ishioka S, Matsumoto T (2002) Effect of fiber concentration and axial ratio on the rheological properties of cellulose fiber suspensions. Nihon Reoroji Gakkaishi 30:27–32

Turbak AF, Snyder FW, Sandberg KR (1983) Microfibrillated cellulose, a new cellulose product: properties, uses, and commercial potential. J Appl Polym Sci Appl Polym Symp 37:815–827

Varanasi S, He R, Batchelor W (2013) Estimation of cellulose nanofibre aspect ratio from measurements of fibre suspension gel point. Cellulose 20:1885–1896

Villay A, de Filippis FL, Picton L, Le Cerf D, Vial C, Michaud P (2012) Comparison of polysaccharide degradations by dynamic high-pressure homogenization. Food Hydrocoll 27:278–286

Wang S, Gao W, Chen K, Xiang Z, Zeng J, Wang B, Xu J (2018) Deconstruction of cellulosic fibers to fibrils based on enzymatic pretreatment. Biores Technol 267:426–430

Xia Z, Li J, Zhang J, Zhang X, Zheng X, Zhang J (2020) Processing and valorization of cellulose, lignin and lignocellulose using ionic liquids. J Bioresour Bioprod 5:79–95

Xu Q, Gao Y, Qin M, Wu K, Fu Y, Zhao J (2013) Nanocrystalline cellulose from aspen kraft pulp and its application in deinked pulp. Int J Biol Macromol 60:241–247

Yu S, Sun, J, Shi, Y, Wang, Q, Wu, J, Liu, J (2020) Nanocellulose from various biomass wastes: its preparation and potential usages towards the high value-added products. Environ Sci Ecotechnol 100077

Zambrano F, Starkey H, Wang Y, de Assis CA, Venditti R, Pal L, Jameel H, Hubbe MA, Rojas OJ, González R (2020) Using micro-and nanofibrillated cellulose as a means to reduce weight of paper products: a review. BioResources 15:4553–4590

Zhang L, Batchelor W, Varanasi S, Tsuzuki T, Wang X (2012) Effect of cellulose nanofiber dimensions on sheet forming through filtration. Cellulose 19:561–574

Zhao H, Kwak JH, Wang Y, Franz JA, White JM, Holladay JE (2006) Effects of crystallinity on dilute acid hydrolysis of cellulose by cellulose ball-milling study. Energy Fuels 20:807–811